ECCOMAS Congress 2016
VII European Congress on Computational Methods in Applied Sciences and Engineering
M. Papadrakakis, V. Papadopoulos, G. Stefanou, V. Plevris (eds.)
Crete Island, Greece, 5–10 June 2016

ON THE MODELING OF SELF-DAMPING IN STRANDED CABLES

Francesco Foti[1]**, Luca Martinelli**[1] **and Federico Perotti**[1]

[1] Politecnico di Milano, Dep. of Civil and Environmental Engineering
P.zza L. Da Vinci 32, 20133, Milano, Italy
e-mail: francesco.foti@polimi.it
luca.martinelli@polimi.it
federico.perotti@polimi.it

Keywords: Self damping, cable dynamics, hysteretic bending, friction.

Abstract. *A new formulation is presented to model the hysteretic bending behaviour of metallic strands. The interaction between the wires of the strand is modeled through a frictional contact model based on the Amontons-Coulomb law and accounts for the effects of the tangential compliance mechanism. The new model is presented with reference to a single-layered mono-metallic strand and is applied to the study of the energy dissipation in cyclic bending.*

1 INTRODUCTION

Overhead electrical lines and, more in general, suspended cable structures subjected to wind forces are typically subjected to aeolian vibration, due to the alternate shedding of Von Karman's vortices. These vibrations can strongly affect the service life of cable structures, by inducing alternate bending stresses leading to wear damage and fretting fatigue of the strands and of the connected support equipment [3]. The assessment of the aeolian vibration level, therefore, is a crucial issue in the design and maintenance of cable supported structural systems.

During aeolian vibration, a relevant fraction of the power transmitted by the wind to the structure is dissipated through frictional dissipation phenomena, which occur within the vibrating cable (also referred to as *cable self-damping*) [3]. Stranded cables, in fact, are made of wires, which tend to slip relatively one to each other during the bending of the element.

An upper bound of the aeolian vibration amplitude can be found by imposing the balance between the input power, provided by the wind, and the total dissipation in the cable structure (Energy Balance Principle, see e.g. [1, 3]). Within this context, the most common approach to estimate the self-damping of the cables is based on experimental measurements on indoor laboratory test spans [4] and empirical or semi-empirical (e.g. [13]) expressions.

Focusing on overhead electrical lines, the following power law is commonly adopted to evaluate the power per unit-length, P_d, dissipated when the conductor vibrates according to a flexural natural mode with amplitude A [m] (single-peak antinode vibration amplitude) and frequency f [Hz]:

$$P_d = k \frac{A^l f^m}{T^n} \tag{1}$$

where: T [kN] is the axial load of the cable (assumed constant over the span) and k is a proportionality factor, depending in general on the mechanical and geometrical properties of the strand (see e.g. [2, 3]). The exponents (l, m, n) of the power law are determined by fitting the experimental data from laboratory forced vibration tests.

The approach based on the empirical power law (1) for the definition of the cable self-damping has two major drawbacks: (a) firstly, it relies on expensive and time consuming laboratory tests, and (b) secondly, it is subjected to quite relevant uncertainties since even small variations in the values of the exponents (l, m, n) can lead to a large scatter in the results of equation (1) (see e.g. [1]).

On the other hand, mechanical models starting from a description of the cable internal structure and of the interaction between wires to determine cable self-damping, up to date are still at the research stage (see e.g. the recent review by Spak et al. [14]).

Recently, the authors proposed a new approach to define the self damping of metallic cables [11], starting from the description of the hysteretic bending behaviour of metallic strands provided in [5, 8, 9]. The relative sliding between wires of a strand is first studied, by modeling each wire as a curved thin rod, according to the classic Kirchhoff-Clebsh-Love structural theory. A kinematic model is defined to relate the generalized strains of the wires to those of the strand and the internal contact conditions are analyzed by neglecting the deformation of the contact surfaces and assuming the classic Amontons-Coulomb friction law. The cross sectional response of the strand under cyclic bending is then studied, to obtain a closed-form expression for the dissipated energy per cycle. The latter turns out to be a non-linear function of the maximum bending curvature reached during the cycle. Furthermore, the dissipated energy depends also on the axial load of the strand and on the friction coefficient of the internal contact surfaces. Finally, once the cross sectional hysteretic bending behaviour is fully characterized, the cable self-damping can be easily evaluated through a straightforward analytical procedure.

The application of this new approach to overhead electrical lines has shown (see [11] for details) that it allows to recover the same structure of the empirical power law introduced in equation (1), while providing a full mechanical interpretation of the exponents (l, m, n) and of the proportionality factor k. The proposed approach has been successfully compared with experimental data from vibration tests on 20-60 m length laboratory test spans. Within this context, it has been shown that the proposed model delivers an upper-bound estimate of the cable self-damping. The latter finding has been recognized as a consequence of the assumption of non-deformable contact surfaces adopted to describe the hysteretic cross sectional behaviour of the strand. Neglecting the tangential compliance of the internal contact surfaces, indeed, can lead to an overestimate both of the dissipated energy per cycle as well as of the maximum bending stiffness of the strand cross section.

The aim of the present paper is to investigate the effect of the tangential compliance mechanism of the internal contact surfaces on the hysteretic bending behaviour of metallic strands. Accordingly, the mechanical model of the strand originally proposed in [5] is extended to account for the effects of the internal relative displacements due to the tangential contact compliance (see also [6]) and applied to evaluate the energy dissipated under cyclic bending loading.

The new mechanical model is presented in this paper with reference to the special case of a single-layered mono-metallic strand, in order to avoid cumbersome calculations stemming from a more complex internal geometry.

2 INTERNAL STRUCTURE OF THE STRAND

A typical structural steel strand is considered in this work. The strand is made of six circular round wires (diameter d_1) wrapped around a straight round core wire (diameter d_0), as it is sketched in Figure 1.

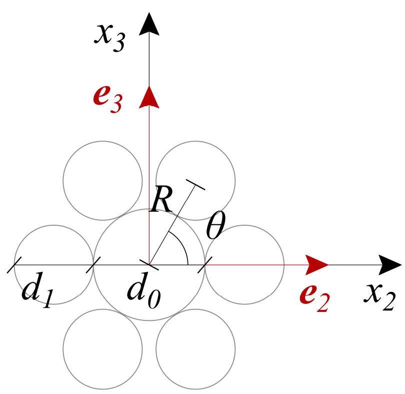

Figure 1: Cross section of the strand.

The external wires are in contact with the core, but not among them. Their centerline can be described as a circular helix in a reference system attached to the strand centerline, with axes $\{x_i\}$ (i=1, 2, 3). The axes x_2 and x_3 are defined on the cross section of the strand, as it is shown in Figure 1, while x_1 identifies the strand centerline. By denoting $\{\mathbf{e}_i\}$ the unit vectors of the axes $\{x_i\}$, the position vector of generic wire centerline can be defined as:

$$\mathbf{x}(\theta)=\frac{R}{\tan(\alpha)}(\theta-\theta_0)\mathbf{e}_1+R\cos(\theta)\mathbf{e}_2+R\sin(\theta)\mathbf{e}_3 \tag{2}$$

where: R is the *helix radius*, which can be simply evaluated as $R=0.5(d_0+d_1)$, α is the lay angle, i.e. the constant angle which the tangent vector to the helix defines with the strand centerline (axis x_1), θ is the *swept angle* defined in Figure 1, and θ_0 denotes the value of the swept angle on the strand cross section identified by the coordinate: $x_1=0$.

3 MODELING OF THE HYSTERETIC BENDING BEHAVIOUR OF THE STRAND

The cross-sectional behaviour of a strand subjected to a combination of axial load F_s and bending moment M_s (herein assumed acting in the plane (x_1, x_3), without loss of generality) can be described through the following constitutive equations (see [5, 6, 8, 9] for details):

$$\begin{cases} F_s = EA_s\varepsilon_s \\ M_s = EI_{\min}\chi_s + M_s^{add}(\varepsilon_s,\chi_s) \end{cases} \tag{3a, b}$$

where ε_s and χ_s are the axial strain and bending curvature of the strand, respectively.

The axial behaviour of the strand (equation (3a)) is linear and independent of the bending curvature. By denoting as EA_0 and EA_1 the axial stiffness of the core and of the external wires, the axial stiffness EA_s can be evaluated (see also [6]) as:

$$EA_s = EA_0 + 6EA_1\cos^3(\alpha) \tag{4}$$

On the other hand, two contributions can be recognized in the expression of the bending moment M_s (equation (3b)). The first one is linear, independent on the axial strain of the strand and accounts for the individual bending of the wires with respect to a diameter parallel to the axis x_2 (see e.g. [8] for details). This term can be evaluated by assuming that the strand behaves as a bundle of individually bent elastic curved thin rods, i.e. by neglecting interaction between the wires of the strand. Under this limit kinematic assumption, the cross sectional bending stiffness attains its minimum value [8]:

$$EI_{\min} = EI_0 + 6\cos^3(\alpha)EI_1 \tag{5}$$

where EI_0 and EI_1 are the bending stiffness of the core and of the external wires, respectively.

The additional term M_s^{add} in equation (3b), instead, is non-linear and accounts for the contribution to the total bending moment of the cross section due to the axial force acting in the individual wires: F_{w1}. The latter, can be decomposed (see also [6]) into a first contribution, $F_{w1,a}$, due to the axial load F_s, and a second one, $F_{w1,b}$, due to the bending of the strand, i.e.: $F_{w1} = F_{w1,a} + F_{w1,b}$. Due to the axial symmetry of the strand, the term $F_{w1,a}$ doesn't depend on the swept angle θ and the additional bending moment in (3b) can be expressed as a function of the components $F_{w1,b}$. The following expression can be easily obtained through equilibrium:

$$M_s^{add} = \sum_{i=1}^{6} R\cos(\alpha)F_{w1,b}(\theta_i)\sin(\theta_i) \tag{6}$$

As long as the friction forces on the internal contact surfaces are large enough to prevent relative displacements (*gross-sliding*) between the wires and the core, i.e. in the *no-sliding* regime, the force $F_{w1,b}$ can be evaluated as:

$$F_{w1,b}^{no-sliding}\left(\theta\right)=\frac{\cos^2\left(\alpha\right)R\;EA_1\;\chi_s}{1+\dfrac{C_{Ti}\left(P\right)EA_1\sin^2\left(\alpha\right)}{R^2}}\sin\left(\theta\right) \tag{7}$$

The above expression accounts for the effect of the internal relative displacements due to the tangential contact compliance mechanism and has been first derived by one of the authors in [6] by extending the mechanical model previously developed in [5] under the assumption of non-deformable contact surfaces.

The variable C_{Ti} in equation (7) is the initial value of the tangential compliance between the external wires and the core, evaluated in the straight configuration of the strand (i.e. for χ_s=0), which depends on the normal force per unit length P exerted from the external wires on the core. The latter, in turn, depends on the axial force acting on the strand and introduces a coupling between the axial problem and the bending of the strand, as already highlighted in equation (3b). Closed-form expressions for the normal contact force P and for the tangential compliance C_{Ti}, here omitted for the sake of conciseness, can be found in [6].

The gradient of the wire axial force $F_{w1,b}$, which can be easily derived from (7), gives the wires the trend to slip with respect to the underlying core. The gross-sliding of the wires, however, is contrasted by the tangential contact forces which act on the internal contact surfaces and are bounded by the Amontons-Coulomb friction law. To study the non-linear transition between the no-sliding and gross-sliding regime, a numerical strategy has been developed by the authors (see e.g.: [5, 9]) and is adopted also in this work. The numerical procedure is based on a classic *Return-Map algorithm*, based on a *no-sliding* prediction and a *gross-sliding* correction. The algorithm delivers the value of the gradient of the wire axial force which satisfies the Amontons-Coulomb friction law, over a discrete set of control points defined along the pitch of the wire. Then, the wire axial force $F_{w1,b}$ is obtained through numerical integration along the wire length.

Once the axial force $F_{w1,b}$ is known, the additional bending moment M_s^{add} can be evaluated from equation (6). Finally, by assuming that the strand is subjected to a bending curvature χ_s cyclically variable in the range $\pm\,\chi_{\max}$, the dissipated energy per cycle can be simply evaluated as the area A_c enclosed in the hysteretic moment-curvature diagrams, i.e.:

$$A_c=\oint_{\pm\chi_{\max}} M_s\left(\chi_s\right)d\chi_s \tag{7}$$

A more detailed discussion on the cross sectional model can be found e.g. in [6] where the results of the implementation into a corotational beam finite element [7, 10] are also presented. The relation between A_c and the dissipated power P_d per unit length of the cable (self-damping), instead, is extensively discussed in [11].

4 NUMERICAL APPLICATION

The proposed model is applied to study the cross sectional hysteretic behaviour of a well-documented steel strand (see e.g. [12, 15]), already studied by the authors under the action of axial load and planar bending in [6, 9]. The geometric and material properties of the element are listed in Table 1.

d_0 (mm)	d_1 (mm)	α (deg)	E (GPa)	ν (-)
3.94	3.73	11.8	188	0.3

Table 1: Geometric and material parameters from [12].

The results obtained with the new formulation proposed in this paper are systematically compared with the predictions of the previous authors' model [5], which neglects the effect of the tangential compliance mechanism (i.e. C_{Ti}=0 in equation (7)). The initial behaviour of the latter model, will be referred to, in the following, as the *full-stick initial behaviour*, to emphasize the fact that in this case the cross section of the strand is initially considered to behave as an ideal rigid body.

Figures 2(a, b, c) show the cross sectional hysteresis loops evaluated for several values of the maximum curvature $\chi_{\max}$. The results have been evaluated for different values of the interwire friction coefficient μ and of the non-dimensional axial load parameter η, defined as the ratio between the axial force F_s and the Rated Tensile Strength of the strand (here 137 kN – see [15]).

From Figures 2(a) and 2(b), it can be easily appreciated that by increasing the strand axial load, the area of the hysteresis loop can be remarkably enlarged. A similar effect is obtained by increasing the value of the friction coefficient (see Figures 2(a) and 2(c)).

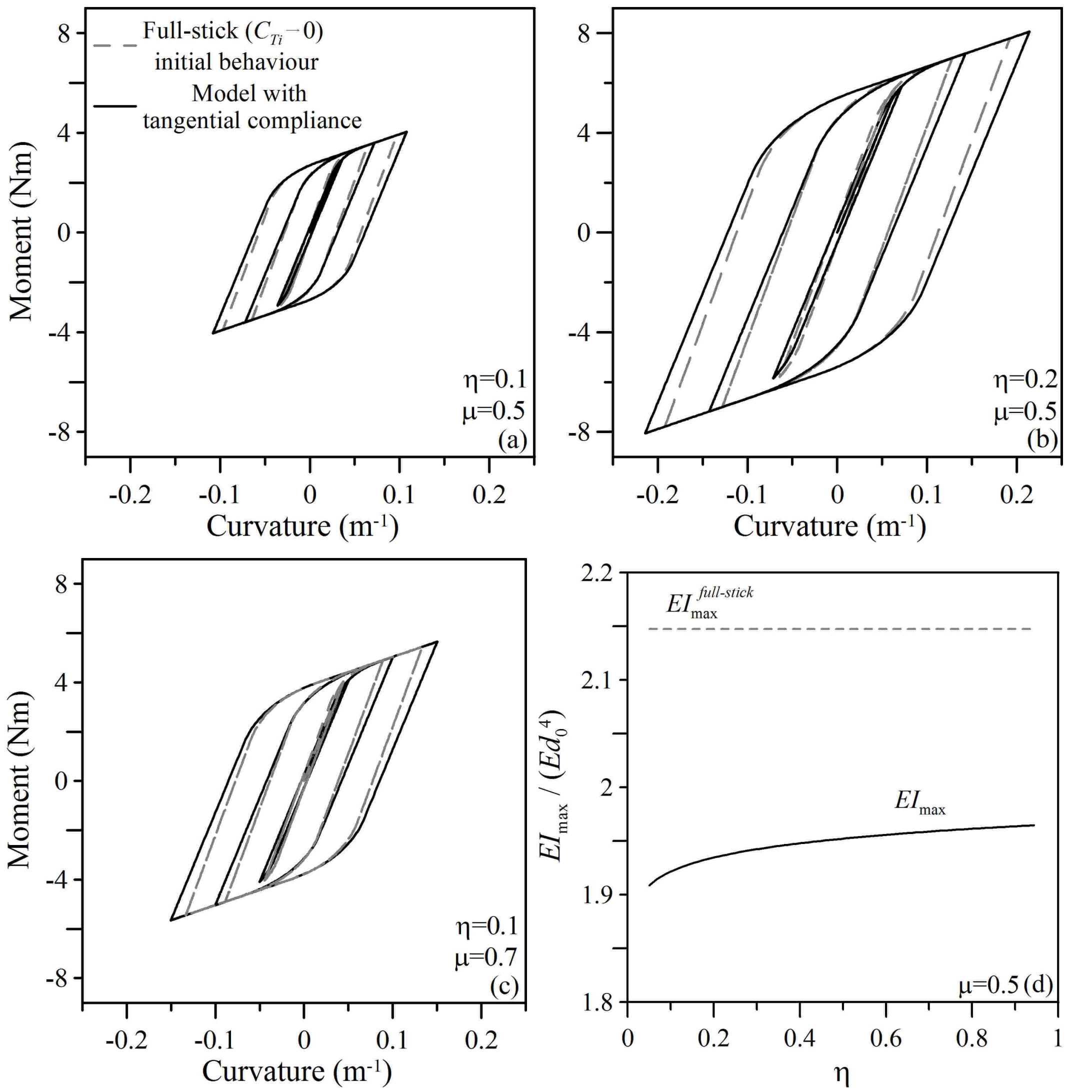

Figure 2: Cross sectional hysteretic behaviour. Hysteresis loops evaluated for: (a) η=0.1 and μ=0.5, (b) η=0.2 and μ=0.5, (c) η=0.1 and μ=0.7. Figure 2(d) shows the non-dimensional initial bending stiffness vs. the axial loading parameter η.

The results of the two models are very similar, for the special case considered in this application. As a matter of fact, the main effect of the tangential compliance mechanism can be recognized in a reduction of about 10% of the value of the initial stiffness of the moment-curvature relation (i.e. the maximum bending stiffness of the strand section: EI_{max}). This effect can be clearly appreciated from Figure 2(d), where the non-dimensional initial bending stiffness $EI_{max}/(Ed_0^4)$ is plotted against the loading parameter η. As a reference, the corresponding constant value evaluated under the full-stick assumption is also plotted with a grey dashed line.

On the other hand, both the area as well as the shape of the hysteresis loops are very slightly affected by the presence of the tangential compliance mechanism. The latter findings can be further appreciated from Figures (3) and (4), where the secant stiffness of the hysteresis loops and the dissipated energy per cycle (see equation (7)), respectively, are plotted against the maximum curvature of the cycles. It's worth noting that, as expected, the dissipated energy per cycle predicted by the new model is always slightly lower than the one evaluated by neglecting the tangential compliance between the external wires and the core.

5 CONCLUSIONS

A new formulation to model the hysteretic bending behaviour of metallic strands has been developed and presented for the special case of single-layered mono-metallic elements. Each wire of the strand is individually modeled as an elastic curved thin rod, in linear contact with the underlying core. A contact model is then introduced to describe the interaction among the external wires and the core. Friction is modeled through the Amontons-Coulomb law and the effects of the tangential contact compliance are accounted for, aiming at extending a previous authors' model taking into account the gross sliding only.

The proposed model, then, has been applied to study the energy dissipation of a steel strand subjected to cyclic bending loading. For the particular strand considered in this work, it is found that the tangential contact compliance mainly influence the initial bending stiffness of the strand, while it has only a small effect on the secant stiffness and area of the hysteresis loops. Ongoing research is devoted to the extension of the proposed formulation to other strand geometries, including the case of multi-layer elements, for which the effects of the tangential compliance are expected to be more pronounced.

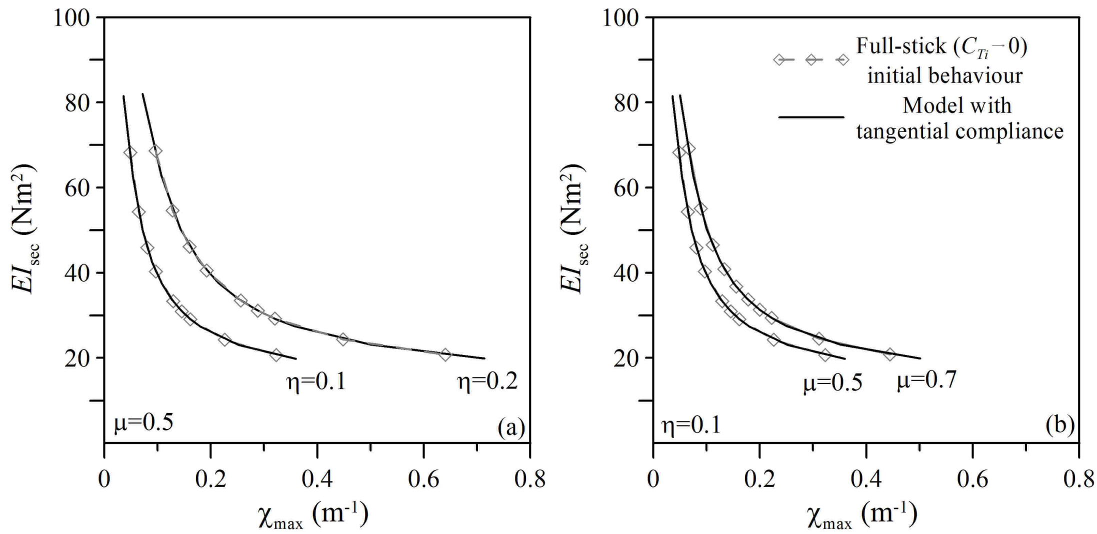

Figure 3: Secant stiffness EI_{sec} of the hysteresis loops vs. the maximum curvature of the cycles χ_{max}. (a) Friction coefficient μ=0.5, different values of η. (b) Axial loading parameter η=0.1, different values of μ.

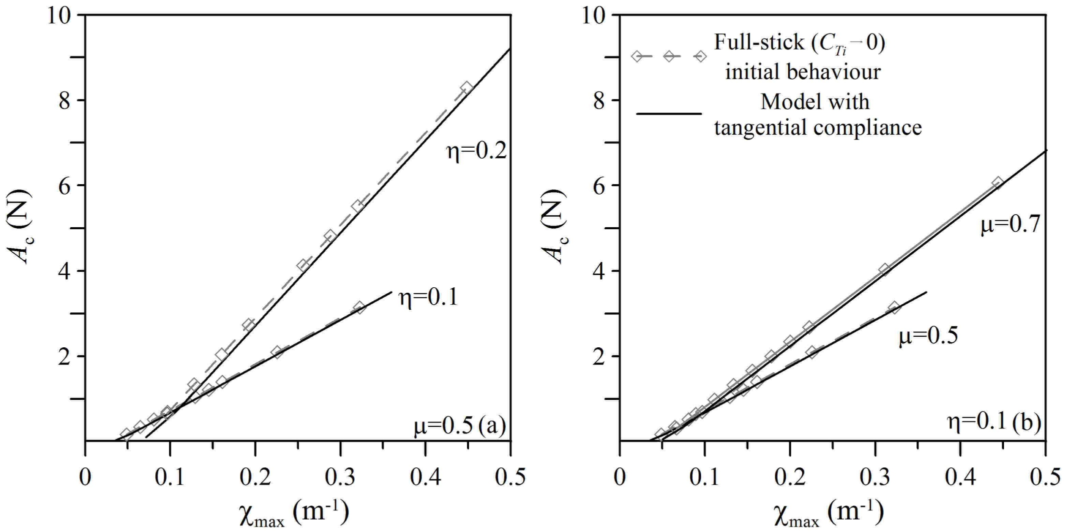

Figure 4: Dissipated energy per cycle A_c vs. the maximum curvature of the cycles χ_{max}. (a) Friction coefficient μ=0.5, different values of η. (b) Axial loading parameter η=0.1, different values of μ.

REFERENCES

[1] CIGRE SC22 WG11 TF 1. Modelling of Aeolian Vibrations of Single Conductors: Assessment of the Technology. *Electra*, **198**, 53-69, 1998.

[2] EPRI, Electric Power Research Institute, Palo Alto CA. *Transmission line reference book- Wind Induced Conductor Motion*, 1979.

[3] EPRI, Electric Power Research Institute, Palo Alto CA. *Transmission line reference book- Wind Induced Conductor Motion*, 2006.

[4] IEEE Power Engineering Society. *IEEE Std. 563.Guide on Conductor Self-Damping Measurements*, 1978.

[5] F. Foti, *A corotational beam element and a refined mechanical model for the nonlinear dynamic analysis of cables*, Doctoral Dissertation, Politecnico di Milano, Milan (Italy), 2013.

[6] F. Foti, A corotational finite element to model bending vibrations of metallic strands. M Papadrakis et al. eds. *Proceedings of the 7th European Congress on Computational Methods in Applied Sciences and Engineering (ECCOMAS)*, Crete Island (Grece), 2016.

[7] F. Foti, L. Martinelli, Dynamics of co-rotational beam elements – some aspects on the kinetic energy and the integration of the equations of motion. J. Eberhardsteiner et.al. eds. *Proceedings of the 6th European Congress on Computational Methods in Applied Sciences and Engineering (ECCOMAS)*, Vienna (Austria), (ISBN:978-3-9502481-9-7) 2012.

[8] F. Foti, L. Martinelli, An analytical approach to model the hysteretic bending behavior of spiral strands, *Applied Mathematical Modelling*. in press (http: //dx.doi.org/ 10.1016/j.apm.2016.01.063), 2016.

[9] F. Foti, L. Martinelli, Mechanical modeling of metallic strands subjected to tension, torsion and bending, Submitted to: *International Journal of Solids and Structures*, 2016.

[10] F. Foti, L. Martinelli, F. Perotti, Numerical integration of the equations of motion of structural systems undergoing large 3D rotations: dynamics of corotational slender beam elements, *Meccanica*, **50**, 751-765, 2015.

[11] F. Foti, L. Martinelli, F. Perotti (2016) A new approach to the definition of self-damping for stranded cables. Submitted to *Meccanica*.

[12] W.G. Jiang, M.S. Yao, J.M. Walton, A concise finite element model for simple straight wire rope strand, *International Journal of Mechanical Sciences*, **41**, 143-161, 1999.

[13] D.U. Noiseux, Similarity laws of the internal damping of stranded cables in transverse vibrations, *IEEE Transactions on Power Delivery*, **7**, 1574-1581, 1992.

[14] K. Spak, G. Agnes, D. Inman, Cable modeling and internal damping developments, *Applied Mechanics Reviews*, **65**, 010801, 2013.

[15] W.S. Utting, N. Jones, The response wire rope strands to axial tensile loads – Part I. Experimental results and theoretical predictions, *International Journal of Mechanical Sciences*, **29**, 605-619, 1987.